Sub-Riemannian Geometry in Image Processing

Alexey Mashtakov
Program System Institute of RAS

Based on joint works with
R. Duits, Yu. Sachkov, E. Bekkers, G. Sanguinetti, A. Ardentov,
I. Beschastnyi, A. Ghosh and T.C.J. Dela Haije

Conference
“Subriemannian geometry and Beyound, II”
Jyvaskyla, Finland, 21.02.2019

SR geodesics on Lie Groups in Image Processing

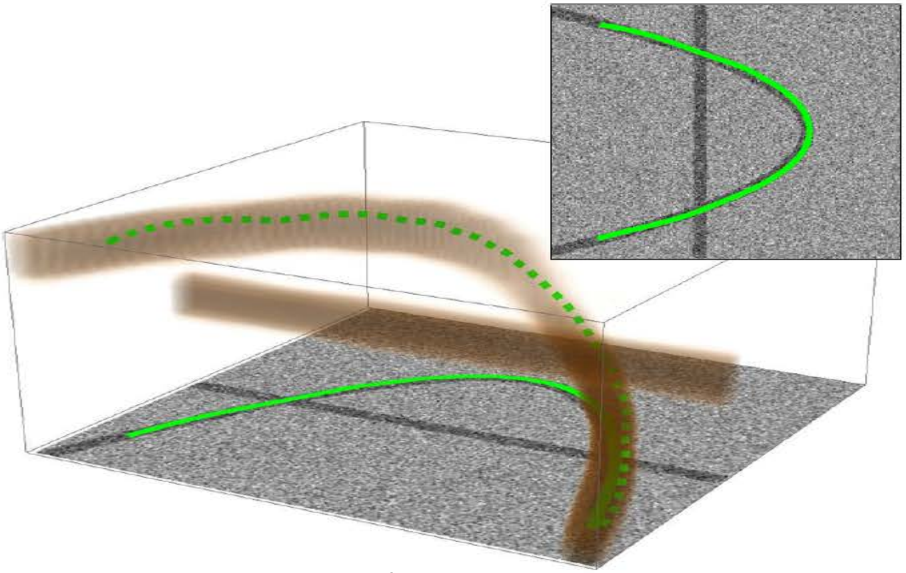

Crossing structures are disentangled

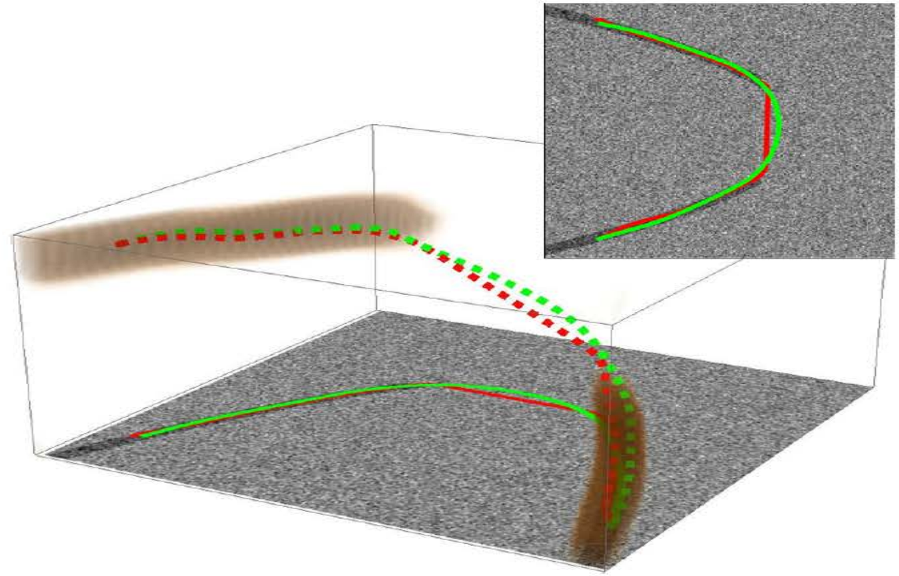

Reconstruction of corrupted contours based on model of human vision

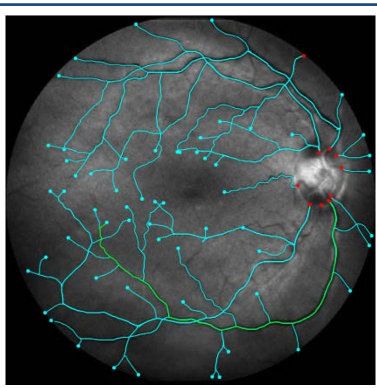

SE(2)

Applications in medical image analysis

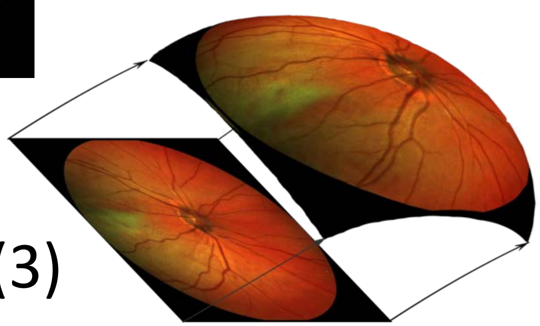

SO(3)

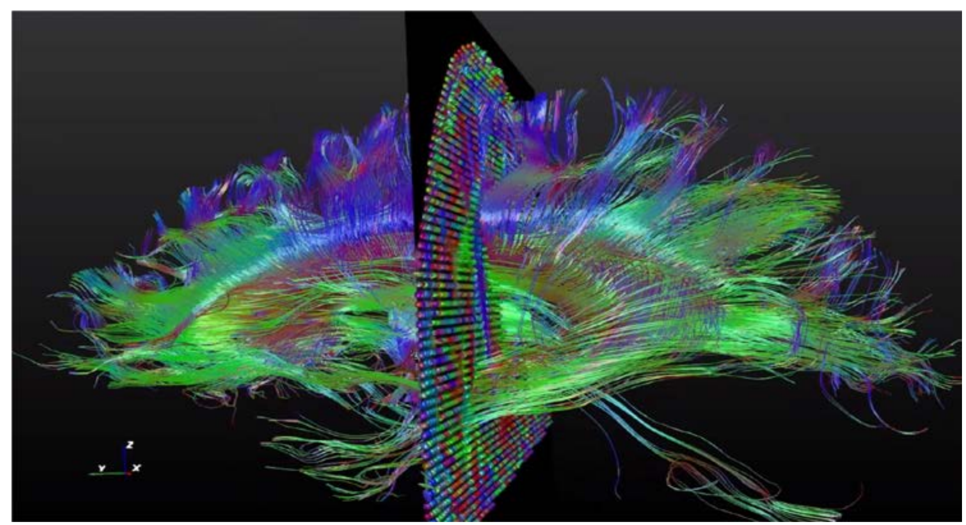

SE(3)

Brain Inspired Methods in Computer Vision

Perception of Visual Information by Human Brain

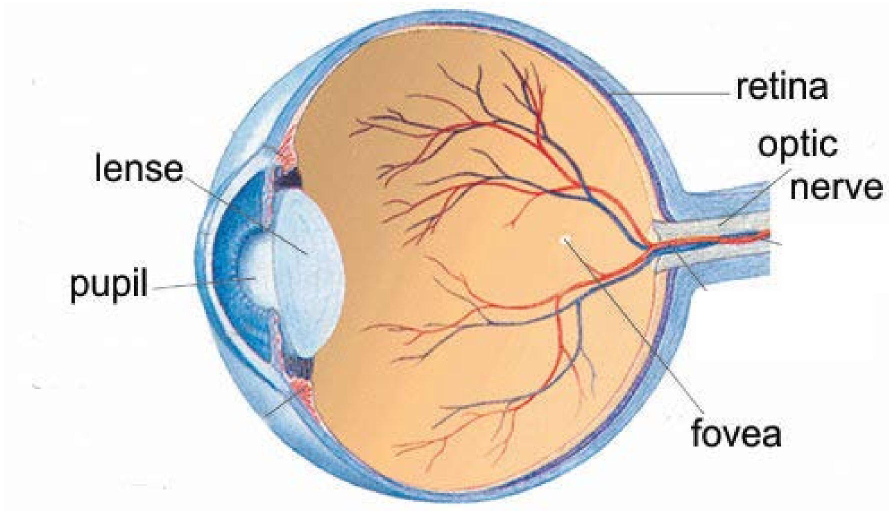

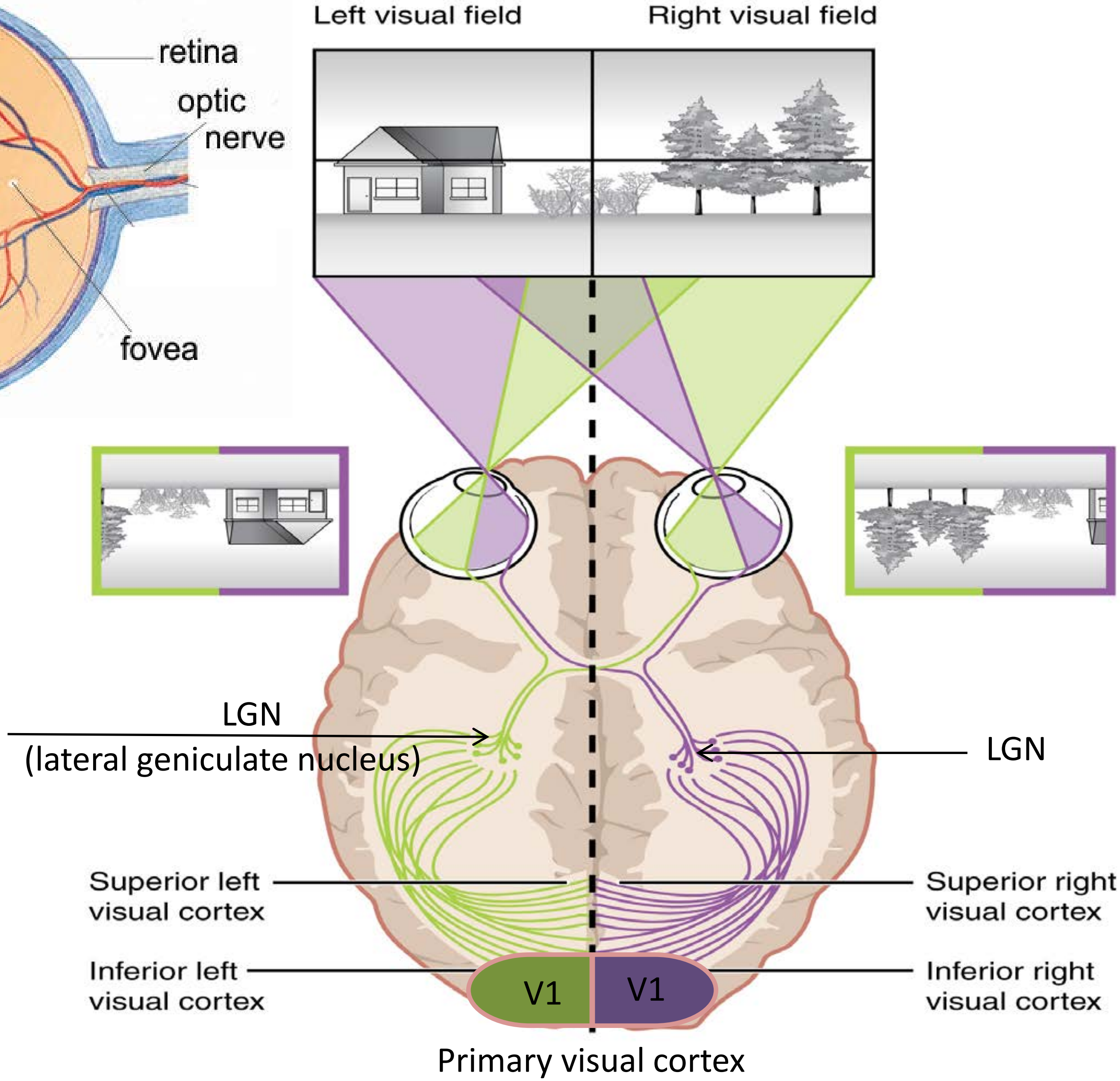

A Model of the Primary Visual Cortex V1

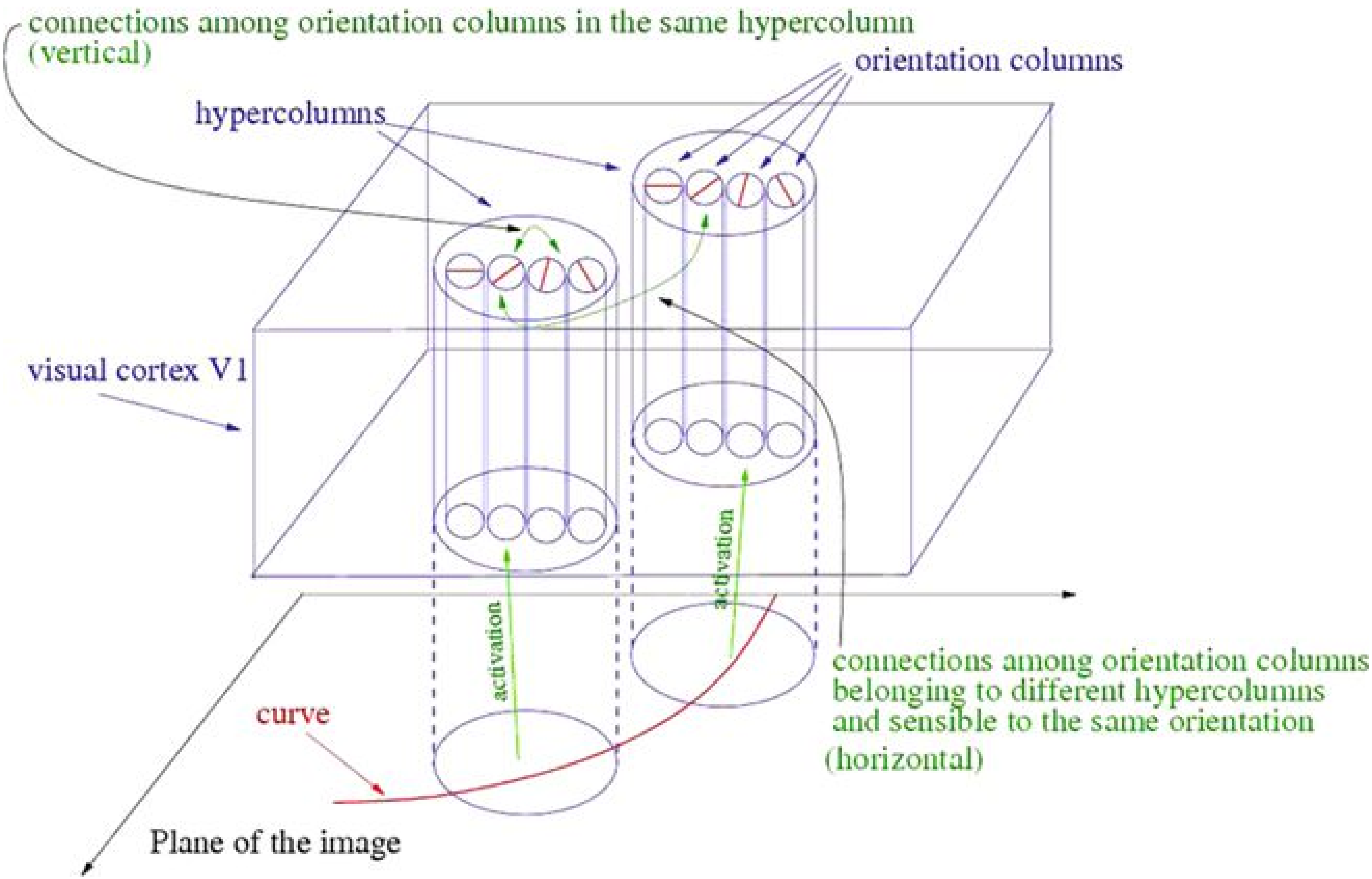

Replicated from R. Duits, U. Boscain, F. Rossi, Y. Sachkov,
Association Fields via Cuspless Sub-Riemannian Geodesics in SE(2), JMIV, 2013.

Cortical Based Model of Perceptual Completion

- D.H. Hubel and T.N. Wiesel, Receptive fields of single neurones in the cat's striate cortex, 1959. Nobel prize in 1981.
- Sub-Riemanian structures in neurogeometry of the vision:
  - J. Petitot, The neurogeometry of pinwheels as a sub-Riemannian contact structure, 2003. (Heisenberg group.)
  - G. Citti and A. Sarti, A Cortical Based Model of Perceptual Completion in the Roto-Translation Space, 2006. ($SE(2)$ group.)
- Variational principle: recovered arc has minimal length in the space (x, y, θ):

$$\int \sqrt{\xi^2 \left(\dot{x}^2 + \dot{y}^2\right) + \dot{\theta}^2 dt} \to \min, \text{ under constraint } \dot{\theta} = \arg\left(\dot{x} + \mathrm{i}\ \dot{y}\right)$$

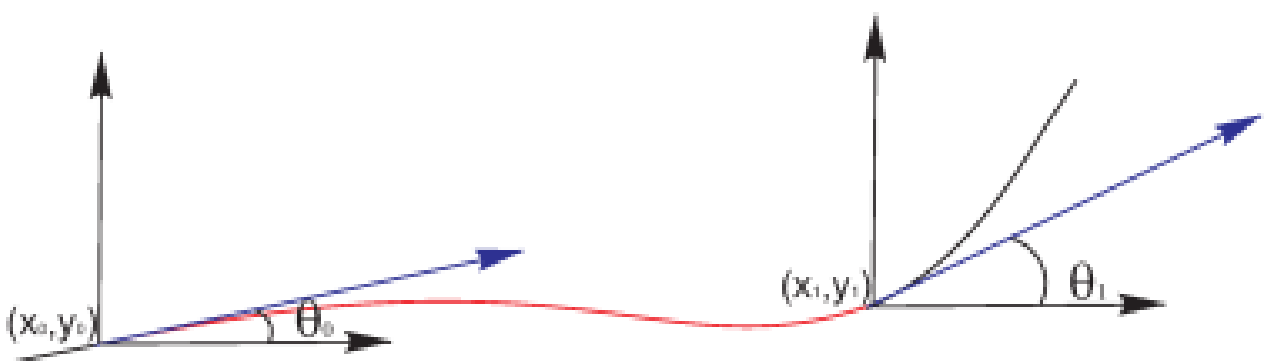

Anthropomorphic Image Reconstruction

By given binary or grayscale image represented as series of isophotes (level lines of brightness) with some corrupted regions to restore the image in a natural (for human eye) way.

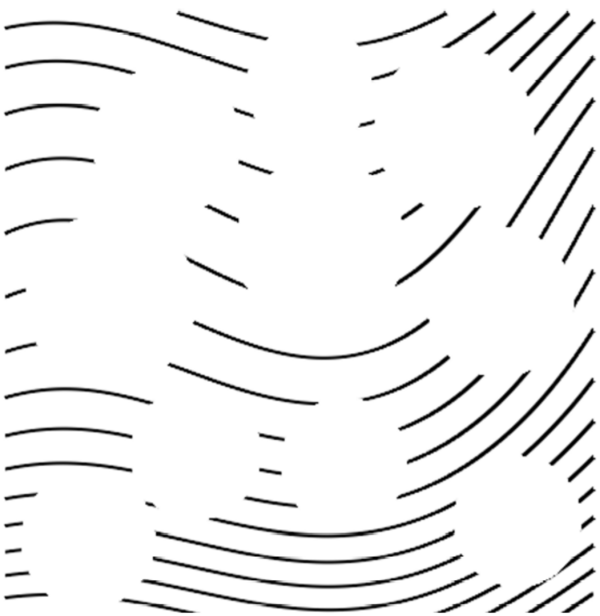

Input (Corrupted) Image

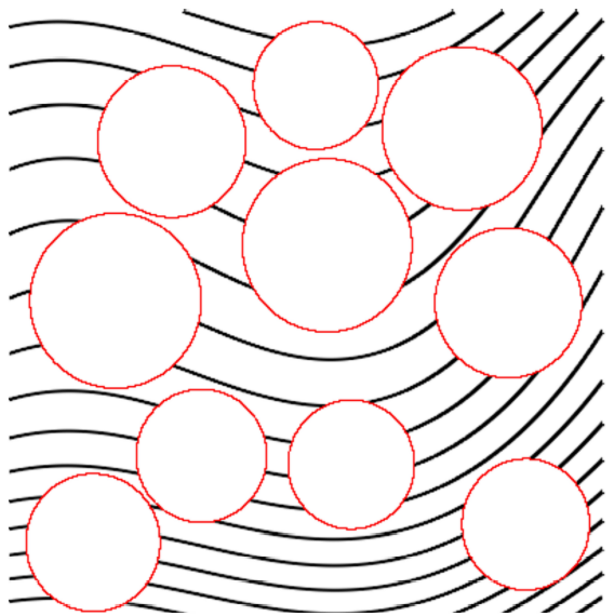

Input Image with Detected Corrupted Regions

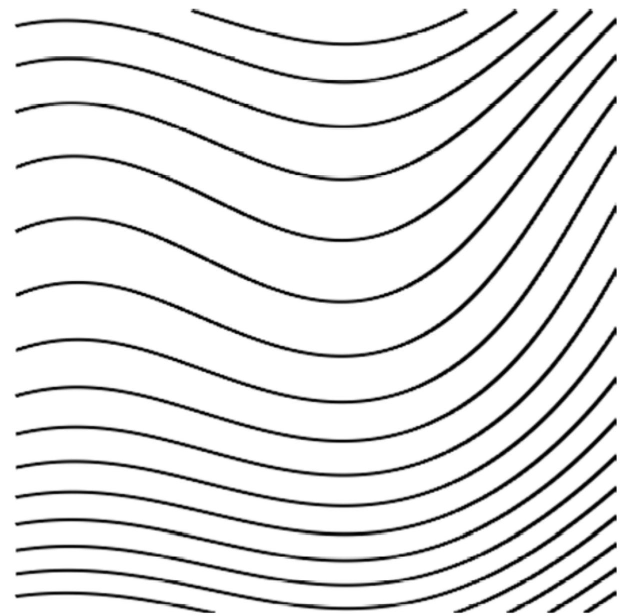

Restored Image

[1] A. Mashtakov, A. Ardentov, Yu. Sachkov, *Parallel Algorithm and Software for Image Inpainting via Sub-Riemannian Minimizers on the Group of Roto-translations*, NMTMA, 2013.

Lie Group Analysis via Invertible Orientation Scores

Image

$f : \mathbb{R}^d \to \mathbb{R}$

Score

$\mathcal{W}_\psi f : G \to \mathbb{C}$

Φ

Processed image

Processed Score

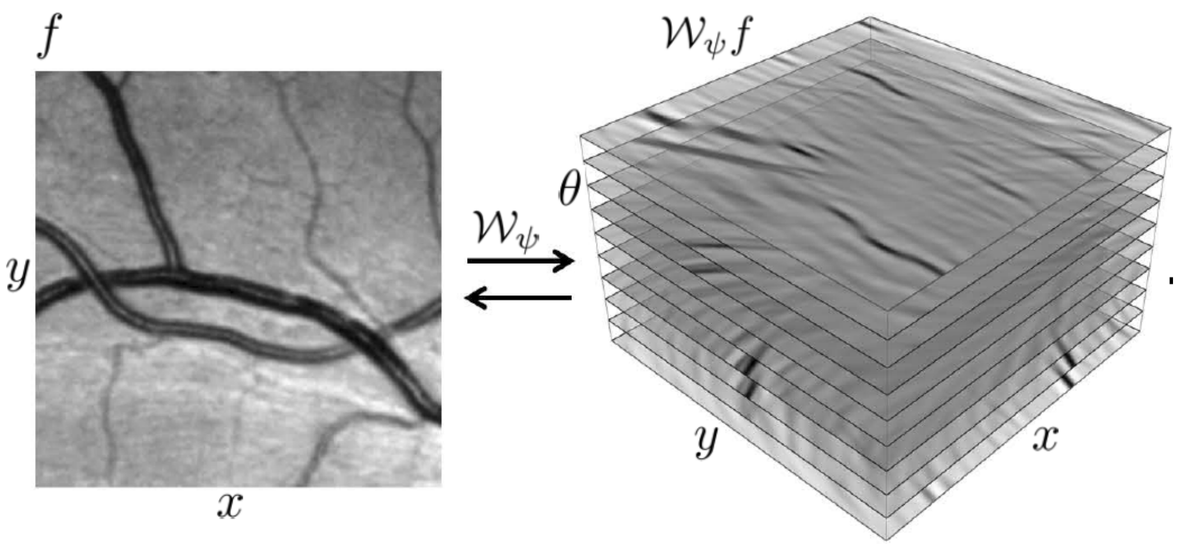

R. Duits: generic mathematical model for contextual image analysis via scores on Lie groups with many applications.

Detection of salient curves in images

Analysis of Images of the Retina

Diabetic retinopathy --- one of the main causes of blindness.
Epidemic forms: 10% people in China suffer from DR.
Patients are found early --> treatment is well possible.
Early warning --- leakage and malformation of blood vessels.
The retina --- excellent view on the microvasculature of the brain.

Healthy retina

Diabetes Retinopathy with tortuous vessels

Geodesic Methods in Computer Vision

Image

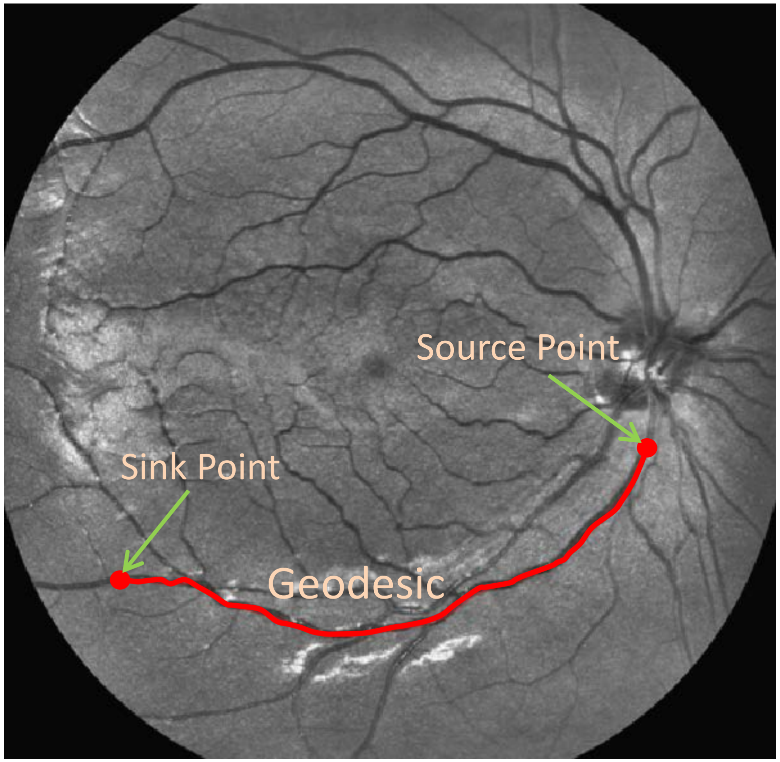

Distance from source point

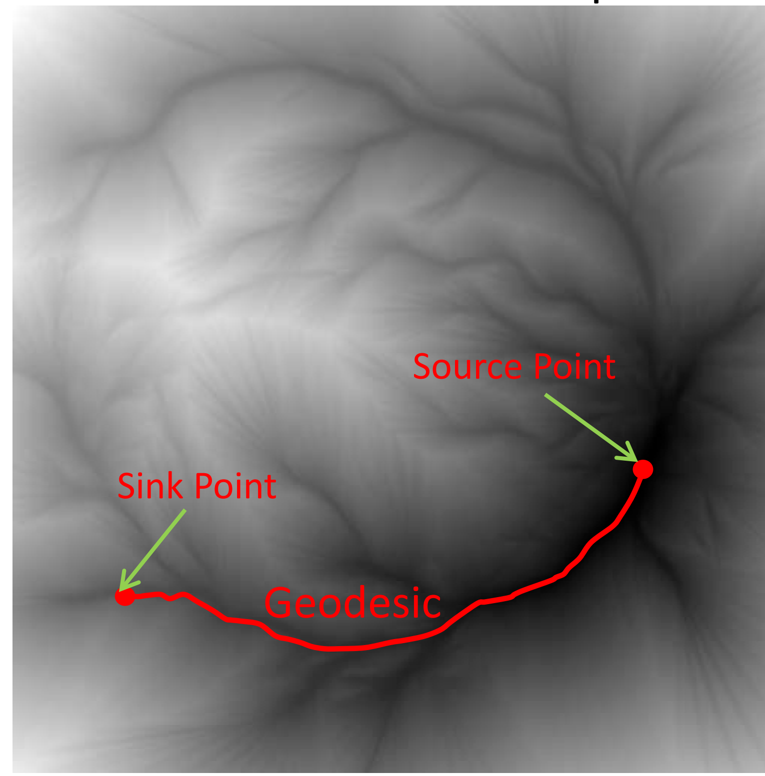

Tracking of salient lines via data-driven minimal paths (or geodesics).

Data-driven Geodesic – curve that minimizes length functional weighted by external cost (function with high values at image locations with high curve saliency).

Fast Marching method to compute geodesics:

1) Computation of distance map from source point,
2) Geodesic via steepest decent on distance map.

Tracking of Lines in Flat Images via Sub-Riemannian Geodesics in SE(2)

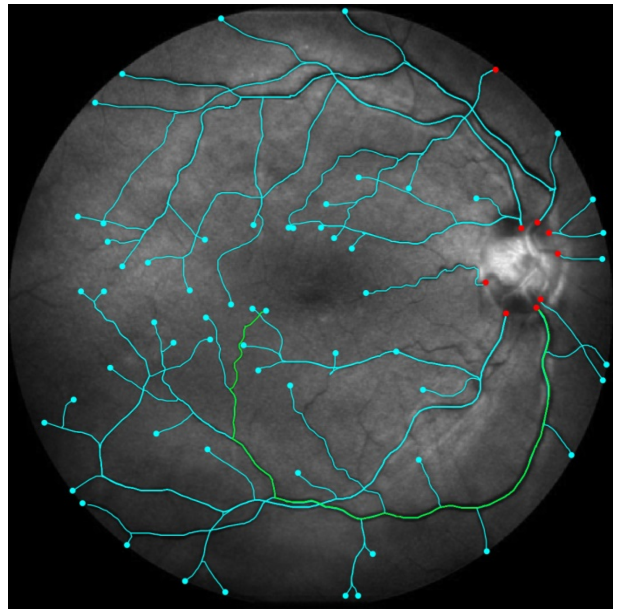

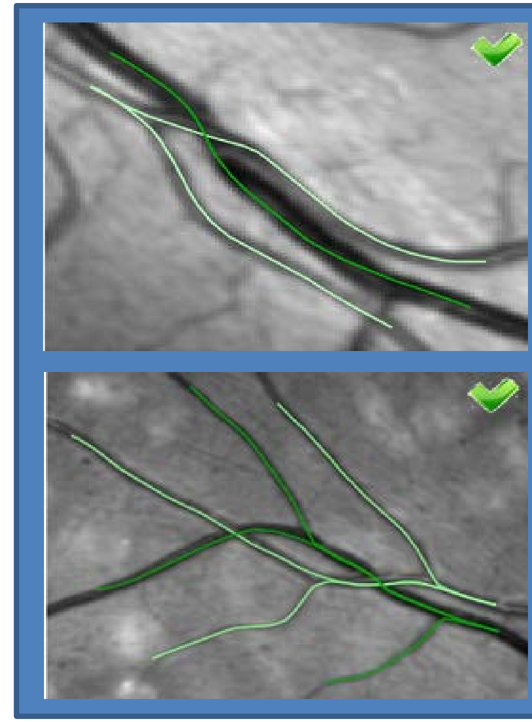

[1] E.J. Bekkers, R. Duits, A. Mashtakov and G.R. Sanguinetti, *Data-driven Sub-Riemannian Geodesics in* SE(2), Proc. SSVM, 2015.

[2] E.J. Bekkers, R. Duits, A. Mashtakov and G.R. Sanguinetti, *A PDE Approach to Data-driven Sub-Riemannian Geodesics in* SE(2), SIIMS, 2015.

[3] G. Sanguinetti, R. Duits, E. Bekkers, M. Janssen, A. Mashtakov, J-M. Mirebeau, *Sub-Riemannian Fast Marching in* SE(2), Proc. CIARP, 2015.

Riemannian Approximation and Fast Marching

Riemannian metric tensor
$$\mathcal{G}_\varepsilon = \mathcal{C}^2(\cdot)\left(\xi^2\omega^1 \otimes \omega^1 + \omega^2 \otimes \omega^2 + \xi^2\varepsilon^{-2}\omega^3 \otimes \omega^3\right)$$

$\varepsilon = 1$

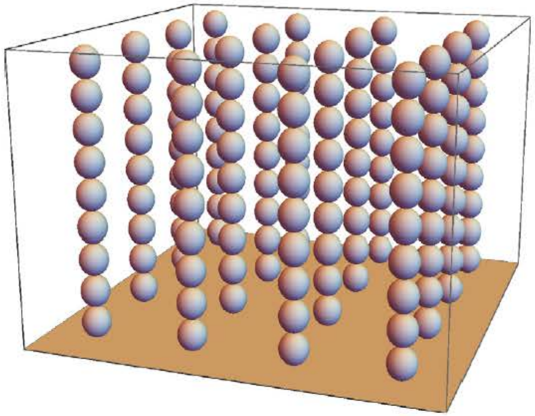

$\varepsilon = 0.1$

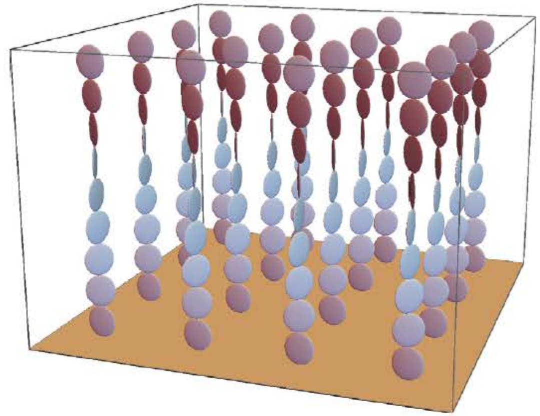

SR Fast Marching for highly anisotropic Riemannian eikonal equation

$$\begin{cases} \text{For } g \neq e: \\ \frac{\mathcal{A}_1|_g(\mathcal{W}_\varepsilon)^2}{\xi^2} + \mathcal{A}_2|_g(\mathcal{W}_\varepsilon)^2 + \varepsilon^2\frac{\mathcal{A}_3|_g(\mathcal{W}_\varepsilon)^2}{\xi^2} = \mathcal{C}^2(g), \\ \text{For } g = e: \quad \mathcal{W}_\varepsilon(e) = 0. \end{cases}$$

Sub-Riemannian metric tensor
$$\mathcal{G} = \mathcal{C}^2(\cdot)\left(\xi^2\omega^1 \otimes \omega^1 + \omega^2 \otimes \omega^2\right)$$

$\varepsilon \to 0$

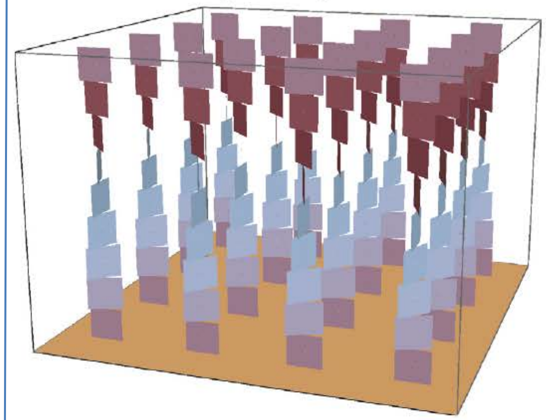

HJB system can be written as SR eikonal equation

$$\begin{cases} \text{For } g \neq e: \\ \frac{\mathcal{A}_1|_g(\mathcal{W})^2}{\xi^2} + \mathcal{A}_2|_g(\mathcal{W})^2 = \mathcal{C}^2(g), \\ \text{For } g = e: \quad \mathcal{W}(e) = 0. \end{cases}$$

[**SDBJMM15**] G. Sanguinetti, R. Duits, E. Bekkers, M. Janssen, A. Mashtakov, J-M. Mirebeau, *Sub-Riemannian Fast Marching in* SE(2), Proc. CIARP, 2015.

Numerical Verification for C=1

Converging to Exact Geodesics

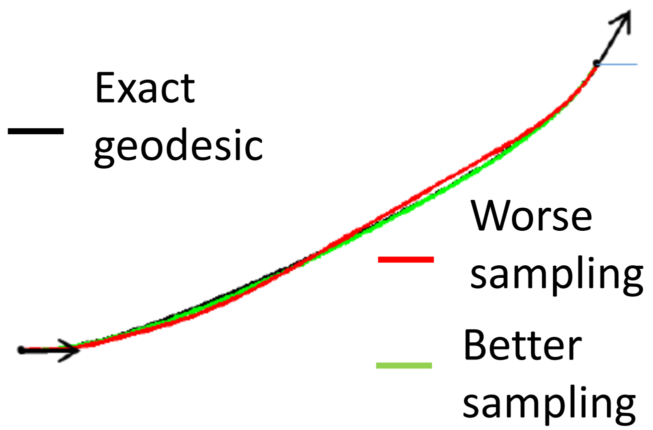

SR-sphere Numerically

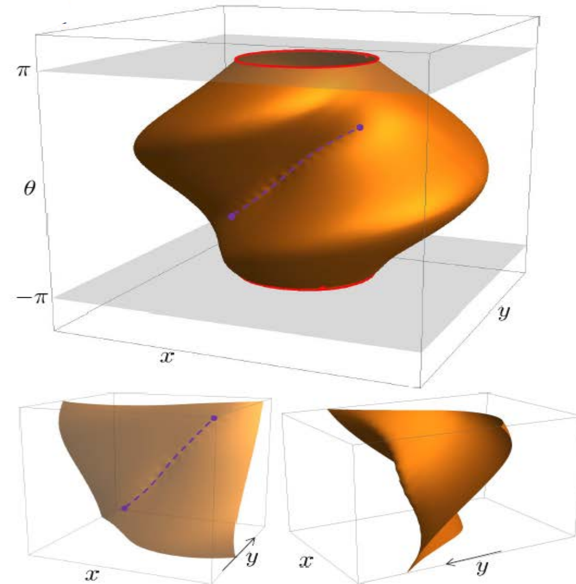

Exact Wavefront

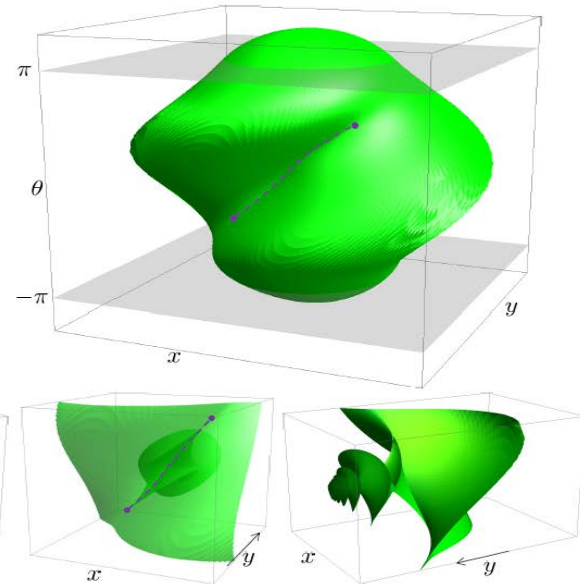

Max Absolute Error

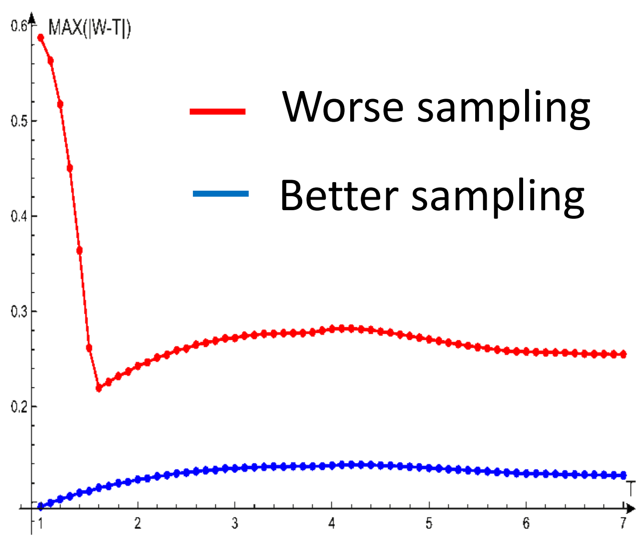

(T – radius of SR-sphere)

Maxwell Set Exact

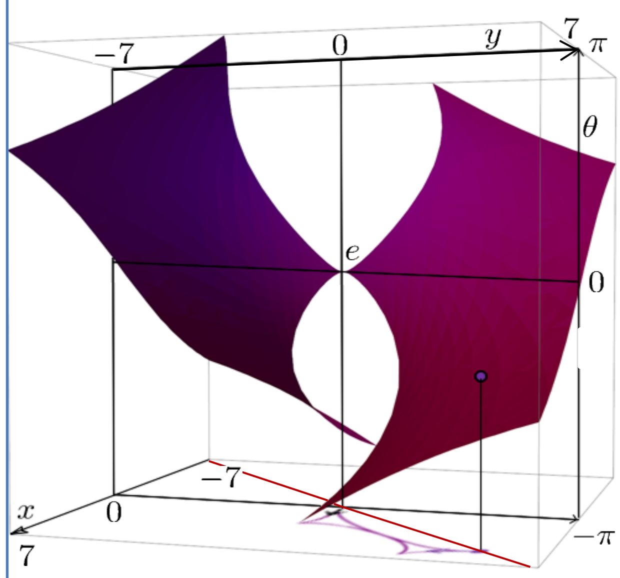

Maxwell Set Numerically

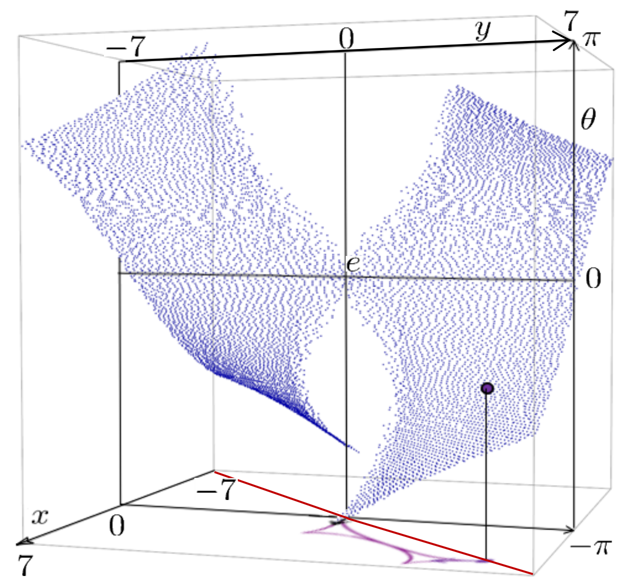

Comparison with Classical Methods

$\mathbb{R}^2$ - Riemannian | $SE(2)$ - Riemannian | $SE(2)$ - Sub-Riemannian

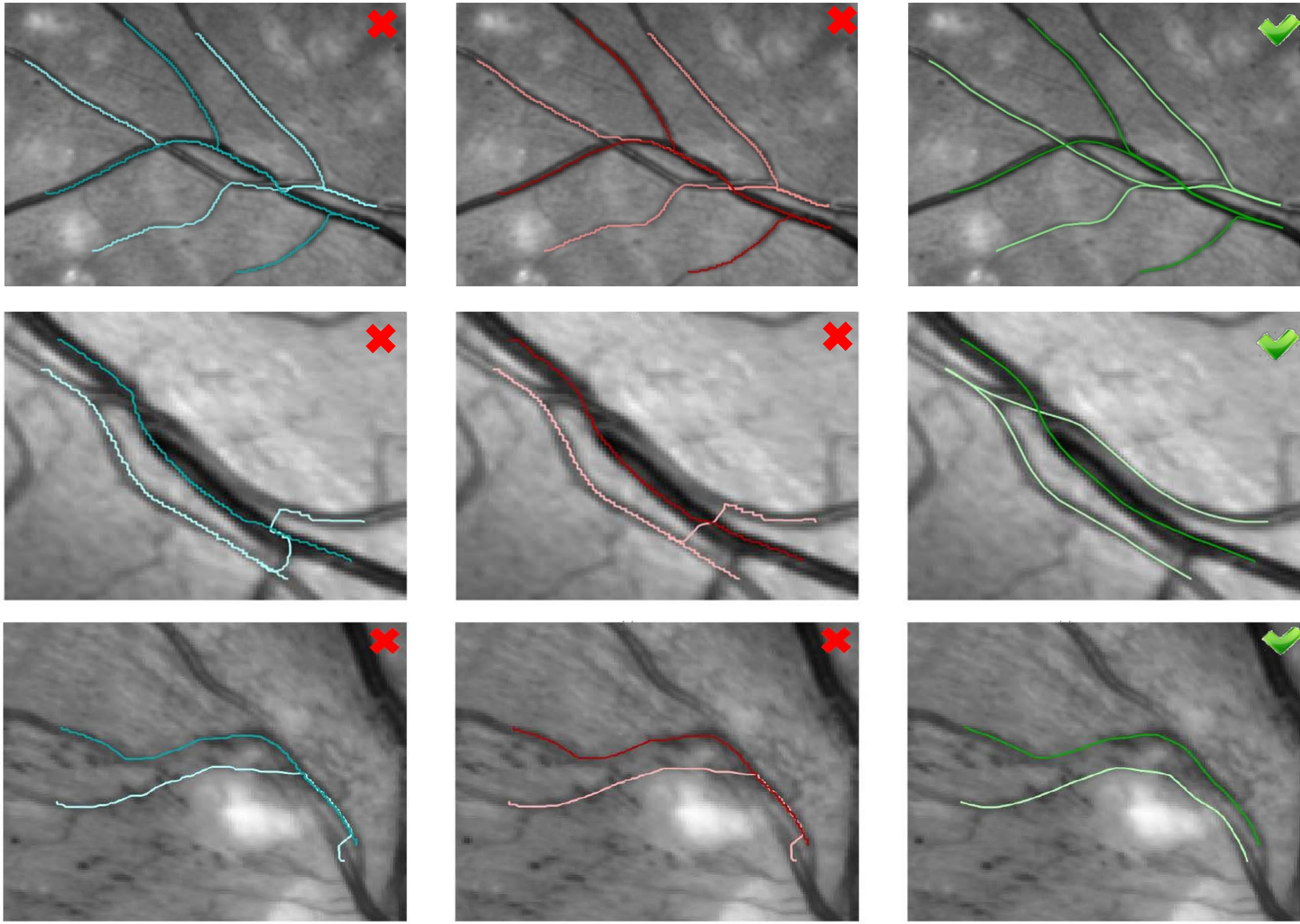

Tracking of Lines in Spherical Images via Sub-Riemannian Geodesics in SO(3)

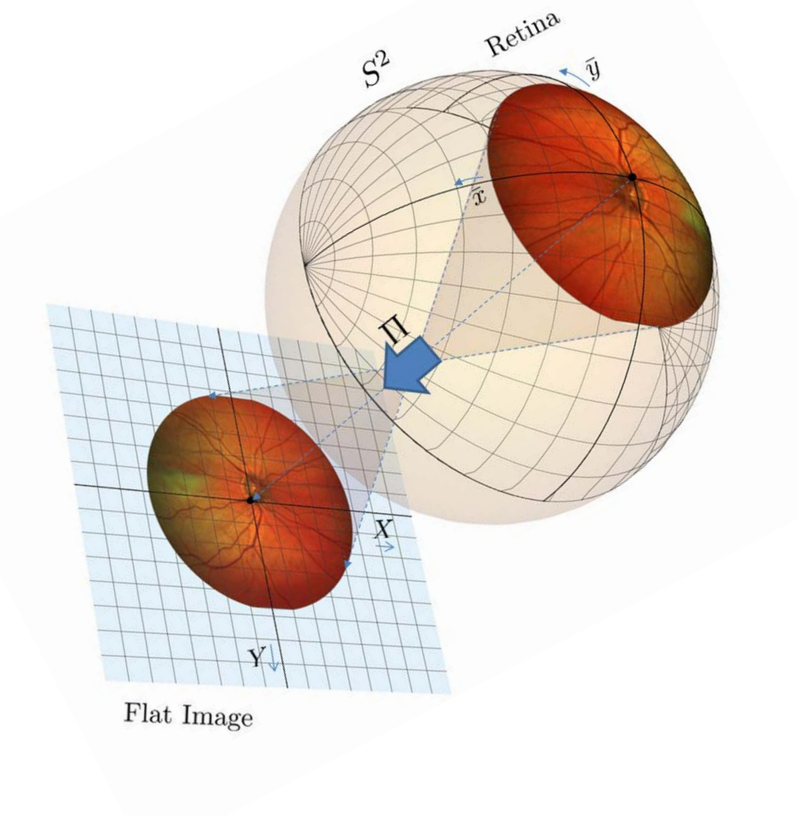

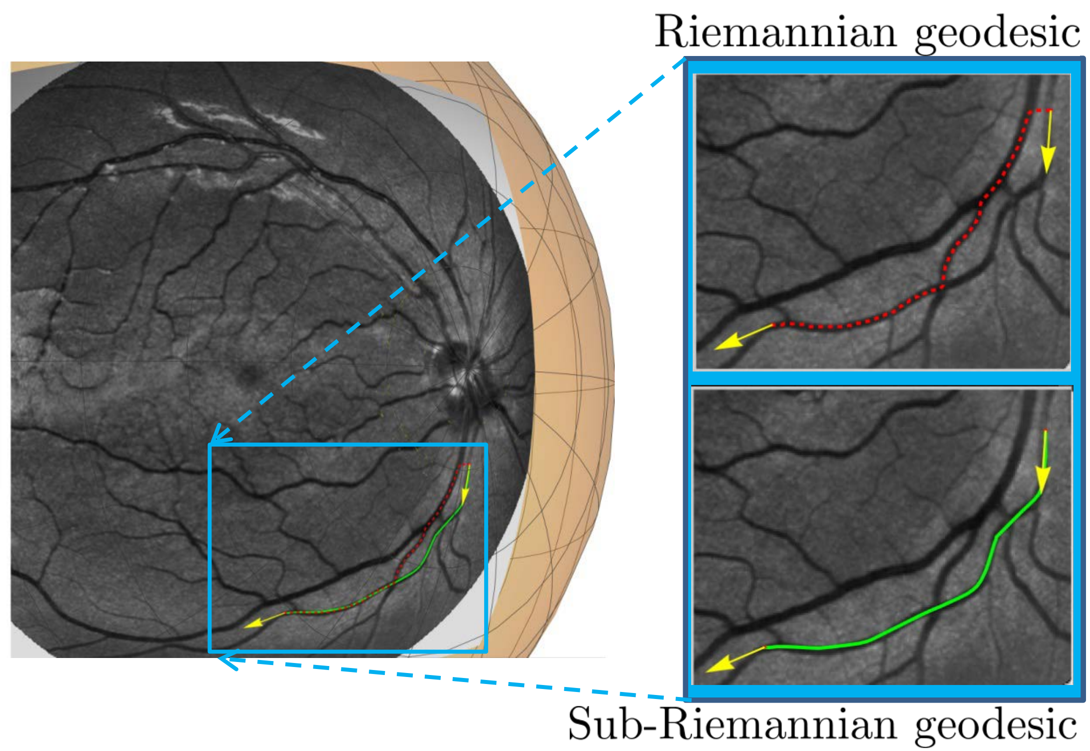

[1] A. Mashtakov, R. Duits, Yu. Sachkov, E.J. Bekkers, I. Beschastnyi, *Tracking of Lines in Spherical Images via Sub-Riemannian Geodesics in SO(3)*, JMIV, 2017.

[2] A.P. Mashtakov, R. Duits, Yu.L. Sachkov, E.J. Bekkers, I.Yu. Beschasnyi, *Sub-Riemannian Geodesics in SO(3) with Application to Vessel Tracking in Spherical Images of Retina*, Doklady Mathematics, 2017.

Sub-Riemannian Fast Marching on SO(3)

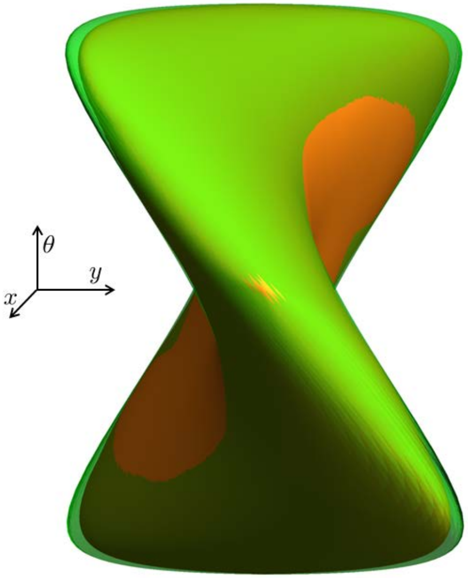

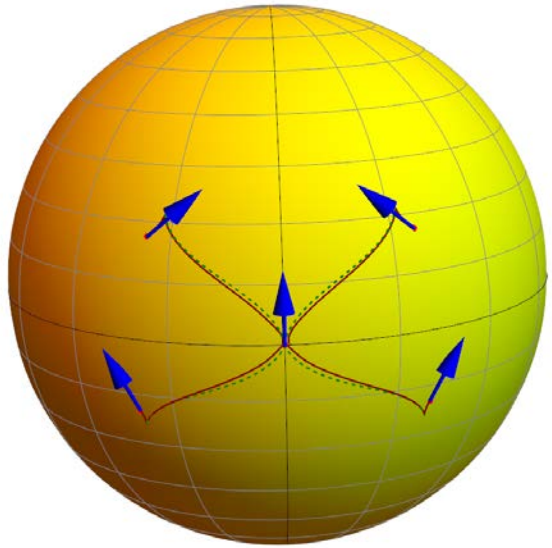

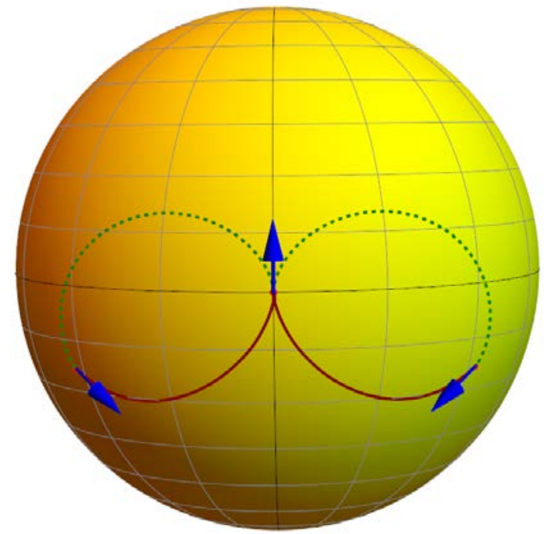

Association Fields via Data-driven SR-geodesics on SO(3)

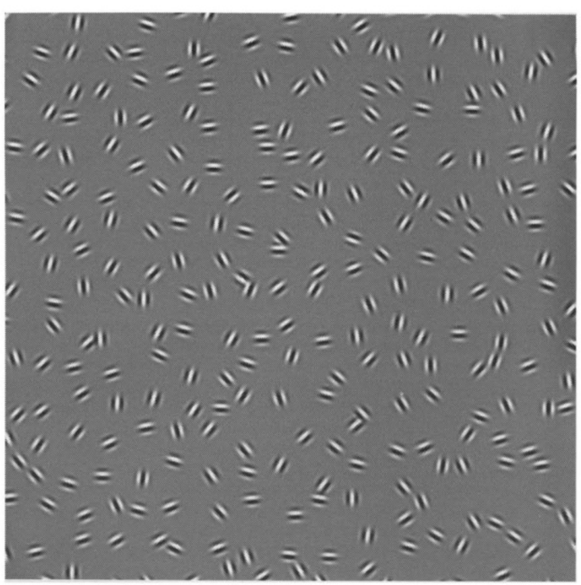

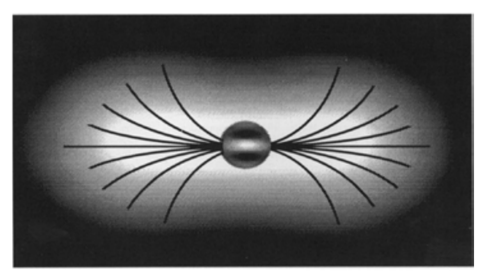

Source: Field et al 1993

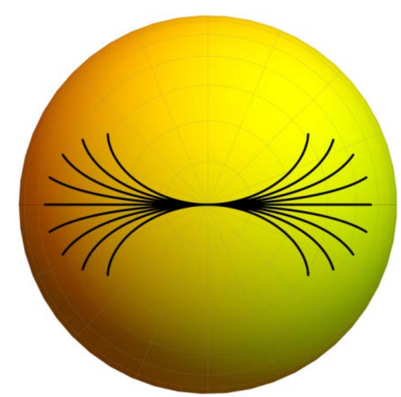

A. Mashtakov, R. Duits. A cortical based model for contour completion on the retinal sphere // PSTA. 2016.

Vessel Curvature via Data-driven SR-geodesics on SO(3)

X_i - l.-i. v.f. on SO(3)

$\mathcal{A}_i$ - l.-i. v.f. on SE(2)

$\gamma^{SO(3)}$ -SO(3) geodesic

$\gamma^{SE(2)}$ - SE(2) geodesic

$\mathcal{W}$ - SR-distance
from source point

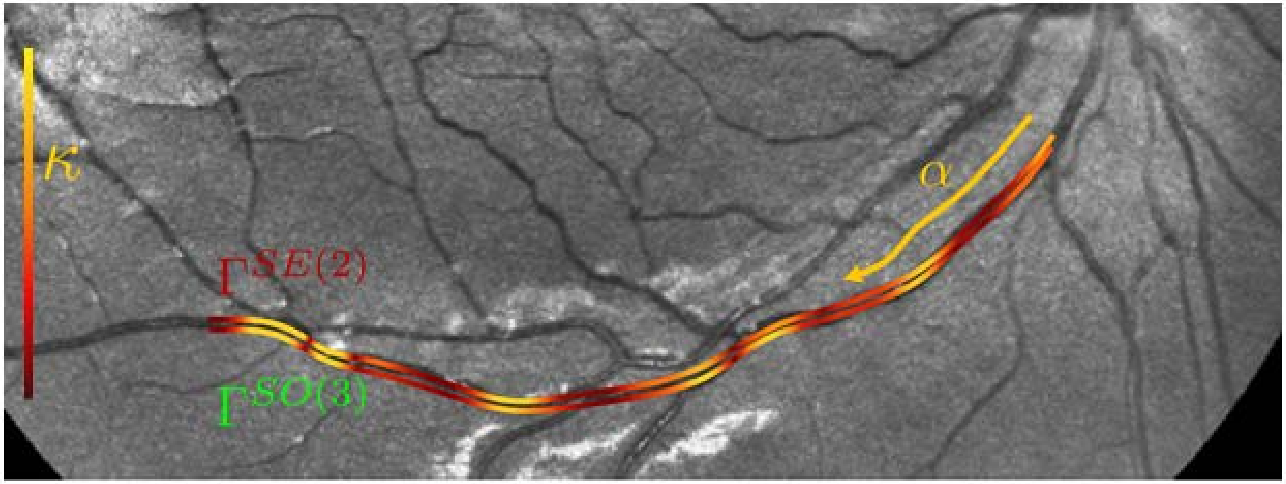

Geodesic curvature

$$\kappa_g^{SO(3)}(\cdot) = \\ = -\xi^2 \frac{X_2|_{\gamma^{SO(3)}(\cdot)}(\mathcal{W}^{SO(3)})}{X_1|_{\gamma^{SO(3)}(\cdot)}(\mathcal{W}^{SO(3)})}$$

Plannar curvature

$$\kappa^{SE(2)}(\cdot) = \\ = -\xi^2 \frac{\mathcal{A}_2|_{\gamma^{SE(2)}(\cdot)}(\mathcal{W}^{SE(2)})}{\mathcal{A}_1|_{\gamma^{SE(2)}(\cdot)}(\mathcal{W}^{SE(2)})}$$

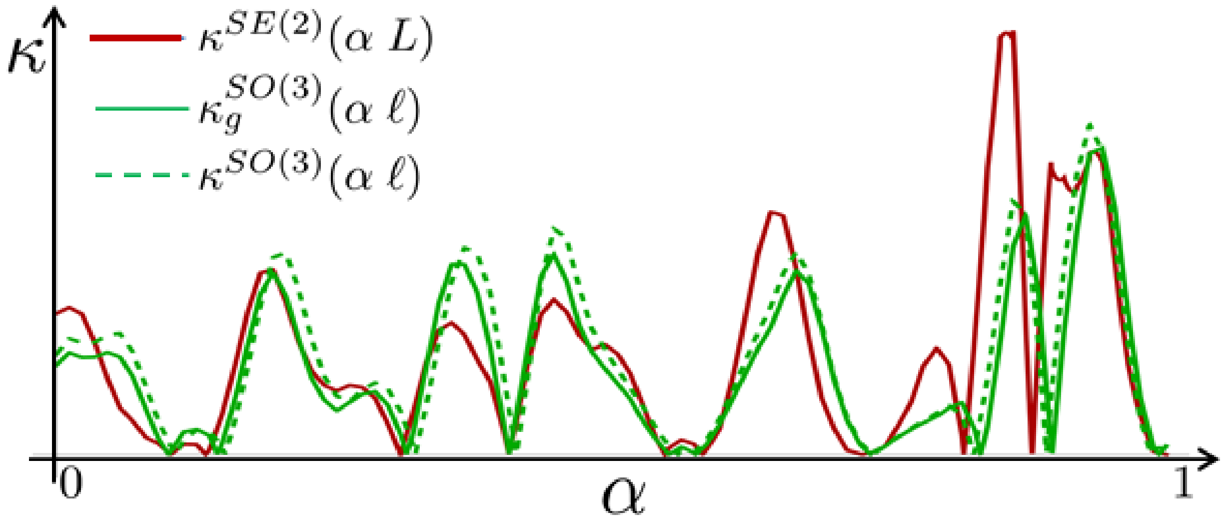

Sub-Riemannian geodesics on SE(3)

Data-driven sub-Riemannian geodesics on **SE(3)** are used for detection and analysis of neuron fibers in magnetic resonance images of a human brain.

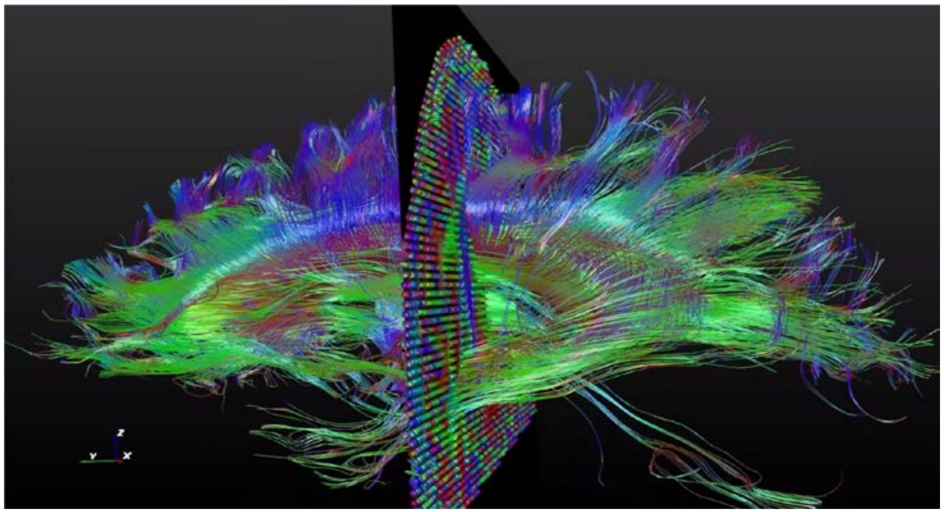

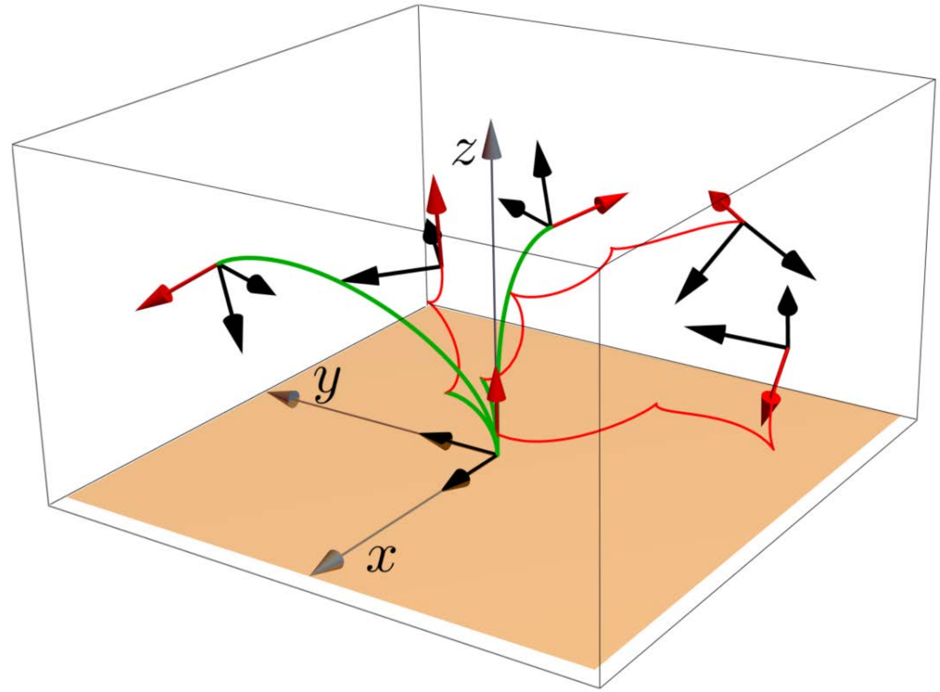

[**1**] R. Duits, A. Ghosh, T. Dela Haije, A. Mashtakov,
On sub-Riemannian geodesics in SE(3) whose spatial projections do not have cusps, JDCS, 2016.

[**2**] A. Mashtakov, A. Popov
Extremal Controls in the Sub-Riemannian Problem on the Group of Motions of Euclidean Space, RCD, 2017.

Sub-Riemannian Fast Marching in SE(3)

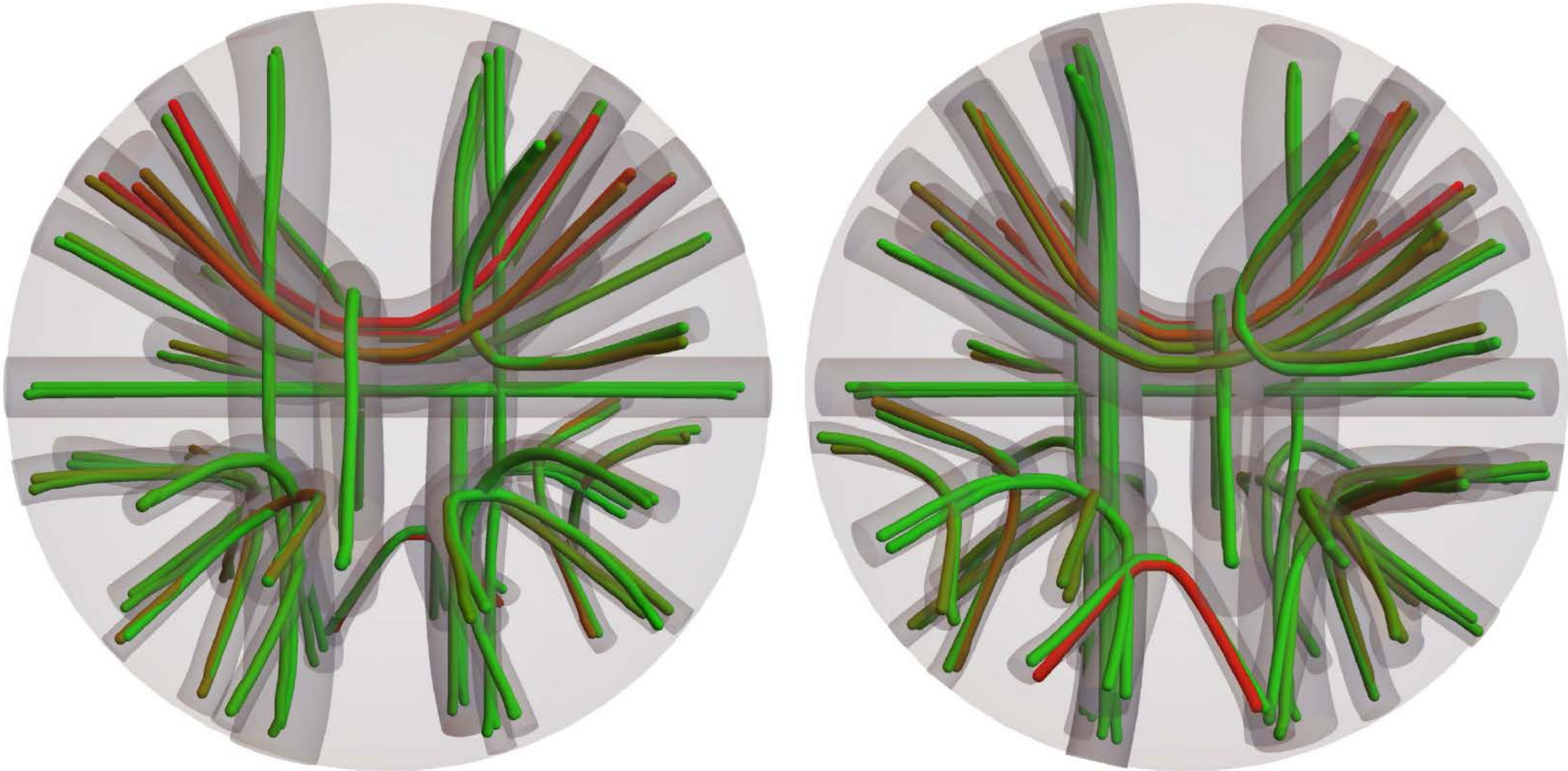

Replicated from J. Portegies, S. Meesters, P. Ossenblok, A. Fuster, L. Florack, R. Duits. Brain Connectivity Measures via Direct Sub-Finslerian Front Propagation on the 5 D Sphere Bundle of Positions and Directions, MICCAI, 2018.

Conclusion

- Sub-Riemannian geometry is a natural tool for brain inspired image processing.
- It is used for athropomorphic image reconstruction.
- And for detection of salient lines and elongated structures in 2D and 3D images.
- Data-driven SR geodesics in SE(2) show promissing results for vessel tracking in flat images of the retina.
- In SO(3) --- in spherical images of the retina.
- In SE(3) --- for fiber tracking in 3D MRI images of human brain.

Thank you for your attention!